ELSEVIER

Silylation of fullerenes with active species in photolysis of polysilane

Takatsugu Wakahara [a], Yutaka Maeda [b], Masahiro Kako [c], Takeshi Akasaka [a,*],
Kaoru Kobayashi [d], Shigeru Nagase [d]

[a] *Center for Tsukuba Advanced Research Alliance, University of Tsukuba, Tsukuba, Ibaraki 305-8577, Japan*
[b] *Department of Chemistry, Tokyo Gakugei University, Koganei, Tokyo 184-8501, Japan*
[c] *Department of Applied Physics and Chemistry, The University of Electro-Communications, Chofu, Tokyo 182-8585, Japan*
[d] *Department of Theoretical Studies, Institute for Molecular Science, Okazaki, Aichi 444-8585, Japan*

Abstract

Organosilicon compounds represent a unique feature of materials such as disilane and polysilane. Meanwhile, since the isolation of C_{60} and C_{70} in preparatively useful quantities, much attention has been devoted to chemical functionalization of these new allotropic forms of carbon, which continuously yields fascinating results. It can be expected that a combination of organosilicon compounds and fullerene forms a new class of organic compounds and at the same time opens a new field in material science. In this context, we have carried out the reaction of fullerenes with active species generated in photolysis of disilane and polysilane, by which we can obtain an attractive material and also clarify the chemical and electronic properties of fullerenes. We here summarize the recent advances in the chemistry of mono- and bis-silylation of fullerenes with silylene and silyl radical to afford the corresponding new fullerene-based organosilicon materials.
© 2003 Elsevier Science B.V. All rights reserved.

1. Introduction

Organosilicon compounds such as disilane and polysilane represent a unique feature of materials [1]. Meanwhile, since the isolation of C_{60} and C_{70} in preparatively useful quantities, much attention has been devoted to chemical derivatization of this new allotropic form of carbon, which continuously yields fascinating results [2]. Exohedrally derivatized fullerenes have been extensively developed to explore their potential usefulness as novel materials. The combination of these two different classes of interesting molecules reveals exciting possibilities for the creation of new types of materials. In this context, we have carried out the reactions of fullerenes with active organosilicon species as silylene and silyl radical generated in photolysis of polysilane. Upon photo-irradiation, they act not only as an attractive synthetic reagent but also as a

mechanistic probe to clarify the chemical and electronic properties of fullerenes. In this account, we would like to briefly summarize our recent results on novel photochemical derivatization of fullerenes with active organosilicon species to afford the corresponding silylfullerenes, [3], which open new routes to synthetically useful derivatization of fullerenes.
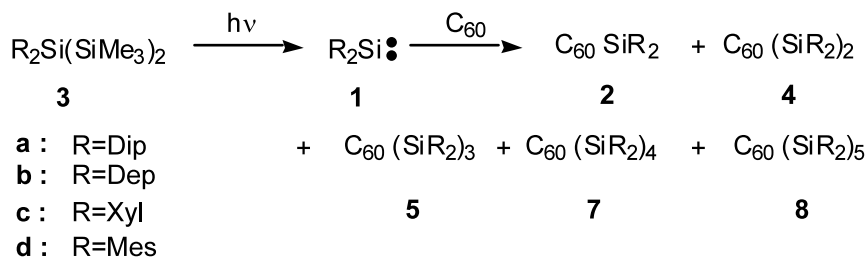
2. Silylation of fullerenes with silylene

2.1. Reaction of C_{60} with silylene

The addition of bis(2,6-diisopropylphenyl)silylene [4] (1a) to C_{60} furnishes the first silylated adduct (2a) as the ring closed 1,2-bridged isomer [5]. Trisilane 3a, a silylene precursor, was photolyzed with a low-pressure mercury lamp in a toluene solution of C_{60}. Purification by chromatography led thermally stable mono-adduct 2a and bis-adduct 4a together with a trace of tris-adduct 5a (Scheme 1). Fast atom bombardment (FAB) mass of 2a displays a peak for 2a as well as for C_{60}, which arises

* Corresponding author. Tel./fax: +81-29-853-6409.
E-mail address: akasaka@tara.tsukuba.ac.jp (T. Akasaka).

$$R_2Si(SiMe_3)_2 \xrightarrow{h\nu} R_2Si: \xrightarrow{C_{60}} C_{60}SiR_2 + C_{60}(SiR_2)_2$$

$$\mathbf{3} \qquad\qquad \mathbf{1} \qquad\qquad \mathbf{2} \qquad\quad \mathbf{4}$$

a : R=Dip
b : R=Dep
c : R=Xyl
d : R=Mes

$$+ \quad C_{60}(SiR_2)_3 + C_{60}(SiR_2)_4 + C_{60}(SiR_2)_5$$

$$\mathbf{5} \qquad\qquad \mathbf{7} \qquad\qquad \mathbf{8}$$

2a'

Dip=2.6-diisopropylphenyl, Dep=2,6-diethylphenyl,
Xyl=2,6-dimethylphenyl, Mes=mesityl

Scheme 1.

from loss of **1a**. The FAB mass, UV–vis and FTIR spectra of **2a** suggest that this new derivative retains the essential electronic and structural character of C_{60}. The ^{13}C-NMR spectrum of **2a** shows a total of 17 signals (4×2; 13×4) for the C_{60} skeleton, suggesting that **2a** has C_{2v} symmetry. The ^{13}C-NMR signal at $\delta = 71.12$, which is ascribed to the sp^3 carbons of the silirane ring, strongly supports **2a** rather than silamethano[10]annulene **2a'**; an sp^2 C–Si should give rise to a signal below $\delta = 130$. This is confirmed by the ^{29}Si-NMR peak at $\delta = -72.74$, since a typical chemical shift for a silicon atom in a silirane ring appears at high field ranging from $\delta = -50$ to -85 [6].

The experimental finding for **2a** was confirmed by AM1 molecular orbital calculations [7] on the reaction of C_{60} and silylenes Ph$_2$Si: and H$_2$Si:, Ph$_2$Si: and H$_2$Si: add across the junction of two six-membered rings in C_{60} to give siliranes **2e** and **2f** (6–6 adducts), with an exothermicity of 61.3 and 78.0 kcal mol^{-1}, respectively (Table 1). The isomeric **2e'** and **2f'** were not found to be

minima on the potential energy surface. The 6–6 adduct **2e** was 19.4 and 10.7 kcal mol^{-1} more stable than the 5–6 adducts **6e** and **6e'**, respectively. **2f** was 19.0 and 6.2 kcal mol^{-1} more stable than the 5–6 adducts **6f** and **6f'**, respectively. The less stable **6e** and **6f** isomerize to **6e'** and **6f'** with a small barriers of 2.0 and 1.0 kcal mol^{-1}, respectively. This is in interesting contrast with the addition of diphenylmethylene for which the 6–6 adduct was calculated to be only 1.2 kcal mol^{-1} more stable than the 5–6 adduct (Fig. 1).

For the silylene addition an interesting feature supporting the formation of several multiple-addition products has been observed in the FAB mass spectra of the reaction mixtures. The product composition of silylene-addition reactions varies with the amount of trisilane used. When an excess of trisilane was used, the corresponding five silylene adducts (**8a**) were also obtained as confirmed by FAB mass analysis. A reason why several silylenes so easily add onto C_{60} is explained by means of AM1 calculations. Table 2 reveals that

Table 1
Relative energies (kcal mol^{-1}) of isomers of C_{60} silylene adduct at AM1 level

	6,6-adduct		5,6-adduct	
	SiR$_2$	SiR$_2$	SiR$_2$	SiR$_2$
	2	**2'**	**6**	**6'**
e : R=Ph	0.0	no minmum	19.4	10.7
f : R=H	0.0	no minmum	19.0	6.2

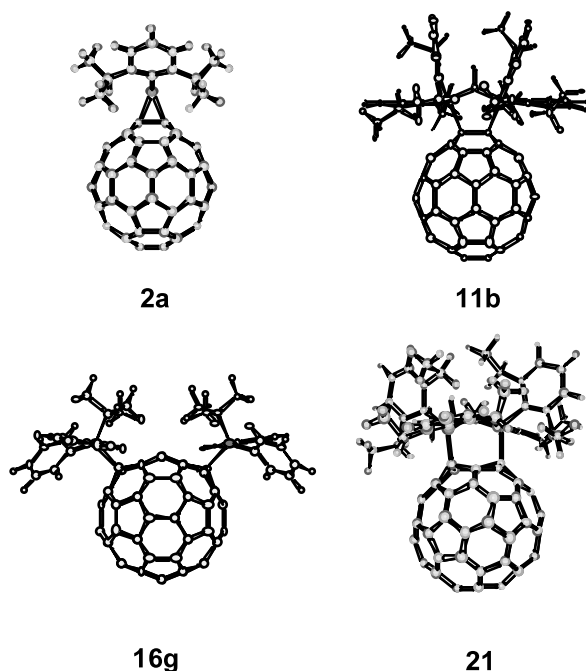**2a**   **11b**

16g   **21**

Fig. 1. View of the structure of **2a**, **11a**, **16g** and **21** calculated with the AM1 method.

there is no significant difference in the heat of reaction for the first, second, third, or even sixth addition of silylene. This result is also confirmed by the charge densities on the diphenyl silylene adduct (**2e**), in which negative charge densities are mainly localized on the sp^3 carbons with only negligible change at other carbon atoms. Almost one electron flows into C_{60}, indicating that **2a** has higher reduction and lower oxidation potentials than C_{60}.

It is known experimentally and theoretically that the reaction of a silylene with olefin is initiated by a nucleophilic $\tilde{\pi}$ approach of the silylene [8]. However, in the present case it was found that silylene electrophilically attacks C_{60} via σ-approach. This might be attributable to the stronger electron accepting ability of C_{60}.

2.2. Reaction of C_{70} with silylene

With the development of the isolation and structure determination of higher fullerenes as C_{70}, the chemical

Table 2
Heat of reaction [a] for the first, second, third, and sixth addition of silylene to C_{60}

| $C_{60}(SiH_2)$	n = 1	n = 2	n = 3	n = 6
[2]H per SiH_2 (kcal mol^{-1})	78.0	(C_s) 77.8	(C_{2v} –A) 77.5	76.9
		(D_{2h}) 77.7	(C_{2v} –B) 77.5	
			(C_1) 77.6	

[a] Calculated at the AM1 level.

reactivity of the higher fullerenes has seen increasing attention and enormous progress has been made. The chemistry of the higher fullerenes may significantly differ from that of C_{60}. It is expected that the silylation of the higher fullerenes would produce a new type of silylfullerenes.

A toluene solution of C_{70} and 2,2-bis(2,6-diisopropyl-phenyl)hexamethyl-trisilane [1] (**1a**) as a silylene precursor was photolyzed with a low-pressure mercury-arc lamp to afford a thermally stable 1:1 adduct (**9**) in high yield as well as the case of C_{60} [9] (Scheme 2). Adduct **9** contains two isomers of Dip_2SiC_{70} (Dip = 2,6-diisopropylphenyl) which were separable by flash chromatography on silica gel. ^{1}H-NMR recorded before chromatography showed that the major (**9A**) and minor (**9B**) isomers form in a 2:1 ratio. FAB mass spectrometry of **9A** displays a peak for **9A** as well as a peak for C_{70} which arises from loss of **1a**. The UV–vis absorption spectrum of **9A** is virtually identical to that of C_{70}. The FAB mass and UV–vis spectra of **9** contain a number of unique features, but also suggest that **9** retains the essential electronic and structural character of C_{70}.

Silylene **1a** adds to C_{60} at the 6-ring–6-ring junctions giving the corresponding silirane [5]. Assuming that **1a** also adds to C_{70} at 6–6 ring junctions, four Dip_2SiC_{70} isomers are conceivable. (Table 3) AM1 molecular orbital calculation [7] on the reaction of C_{70} and dihydrosilylene shows that the 6,6-adduct is more stable than the 5,6-adduct. In these four isomers, the silyl groups are positioned differently with respect to the mirror planes of C_{70} such that they each correspond to a characteristic number of symmetry independent carbons and protons. (Table 3, Fig. 2) The ^{1}H-NMR spectrum of **9A** displays four methyl signals, and two methine signals. Similarly, four methyl signals, and two methine signals are observed in the ^{1}H-NMR spectrum of **9B**. The ^{13}C-NMR spectrum of **9A** shows two signals for the C_{70} skeleton which are attributed to the sp^3 fullerene carbons. Comparing the NMR data for the two isomers, **9A** and **9B**, with the number of possible peaks for a,b-, c,c-, d,e- and e,e-isomers, **9A** and **9B** correspond to a,b- and c,c-isomers, respectively (Table 3).

The chemical shifts of the two sp^3 carbon signals, and the silicon signal are fully consistent with those expected for the silirane carbon atom and silicon atom in **9A** rather than in the isomeric silamethanoannulene **10a** [5]. This experimental finding is also supported by AM1 calculation [7] on the reaction of C_{70} with **1a** which shows that **10a** is not located on the potential energy surface.

The kinetically controlled regioselectivity observed for the addition of silylene **1a** to C_{70} agrees qualitatively with the AM1 calculation on C_{70} in that addition occurs at the a–b and c–c bonds having high bond order [10,11]. Remarkably, the major kinetic product of silylene addition is **9A** in which the silylene adds to the
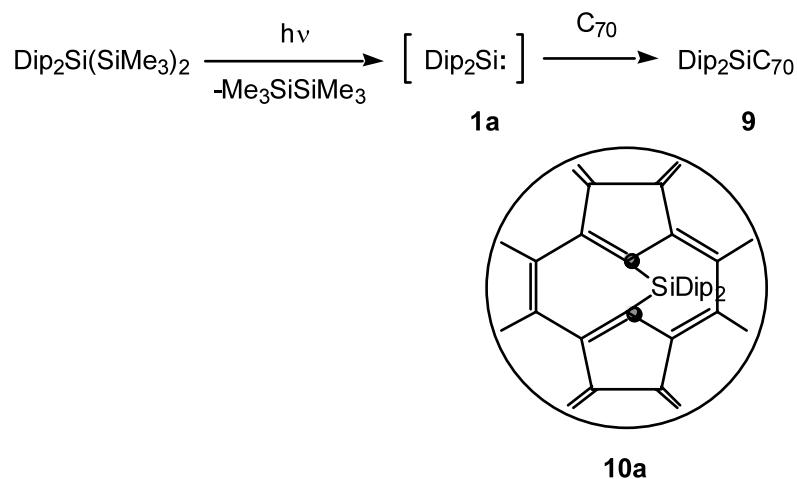
Scheme 2.

Table 3
Number of independent protons and carbons in the 6–6 adduct of Dip_2SiC_{70} (9)

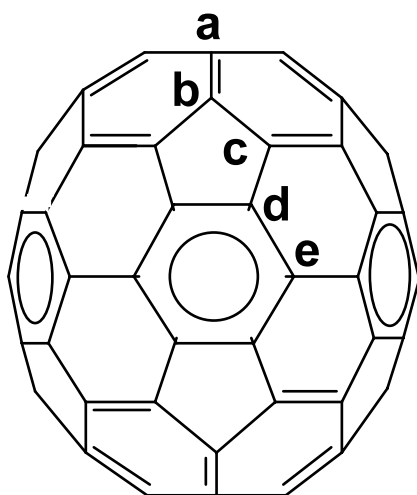| Isomer	Symmetry	CH	CH₃	sp³ carbon on C_{70}
9A	C_s	2	4	2
9B	C_s	2	4	1
a,b-	C_s	2	4	2
c,c-	C_s	2	4	1
d,e-	C_1	4	8	2
e,e-	C_{2v}	1	1	1

Fig. 2. Five distinct carbons, a–e, in C_{70}.

6–6 ring junction at the a–b bond. The isomers do not equilibrate under the reaction conditions; silylation is kinetically controlled.

Products **9A** and **9B** are calculated to lie almost same in energy; **9A** and **9B** are formed with an exothermicity of 46.3 and 46.4 kcal mol⁻¹. Moreover, the ratio of isomers **9A** and **9B** (2:1) is not correlated with the calculated bond orders for the respective bonds in C_{70},

1.480 and 1.526 [11]. In contrast to the exothermicity for the addition of **1a** to C_{70} and bond orders, the magnitude of the LUMO electron densities of C_{70} at the HF/3-21G level agrees well with the observed regioselectivity. The LUMO electron densities at the positions a, b and c in C_{70} are 0.10, 0.05 and 0.05, respectively. Thus, addition of silylene onto C_{70} takes place mainly at the a–b bond and to a lesser extent at the c–c bond reflecting that the HOMO(silylene)–LUMO(C_{70}) interaction plays an important role in the reactivity of C_{70}. In conclusion, spectroscopic analysis and theoretical investigation strongly support that addition at the a–b double bond at the poles is more favorable than that at the c–c bond, and the adducts have the silirane structure **9** and not the isomeric 1,6-silamethano[10]annulene structure **10a**.

2.3. Redox properties of silylene adducts

To design new organofullerenes for applications in material science and biochemistry, one should know how the substituents on C_{60} affect its electronic properties. Namely, an interesting point is how the silicon groups on C_{60} affect its redox properties. The relationship between the structures and redox properties was investigated by a comparative electrochemical study of various organofullerenes derivatized with oxygen-, carbon-, and silicon containing groups at a 6,6-ring junction [12]. A characteristic feature of the mono-silylated and bis-silylated fullerenes is their higher reduction and lower oxidation potentials than C_{60} itself and analogous carbon substituted derivatives, due to the electron releasing nature of silicon relative to carbon. AM1 molecular orbital calculations [7] were carried out on selected organofullerenes to examine the linear correlations of the redox potentials with MO energy levels. The first and second reduction potentials correlate well with the LUMO energy levels, while the third

Table 4
Half-wave potentials of C_{60} and organofullerenes by cyclic voltammetry [a]

Compound	oxE1	redE1	redE2	redE3
C_{60}	+1.21	−1.12	−1.50	−1.95
12		−1.23	−1.58	−2.11
11b	+0.77	−1.24	−1.62	−2.13
13		−1.18	−1.56	−2.03
2a	+0.65	−1.26	−1.63	−2.18
C_{70}	+1.21	−1.10	−1.46	−1.86
9A	+0.59	−1.22	−1.59	−2.02
9B	+0.61	−1.24	−1.58	−1.97
14	+1.12	−1.05	−1.44	−1.84

[a] Values are relative to ferrocene/ferrocenium couple.

11b **12** **13**

R=CH$_2$CO$_2$Et

14
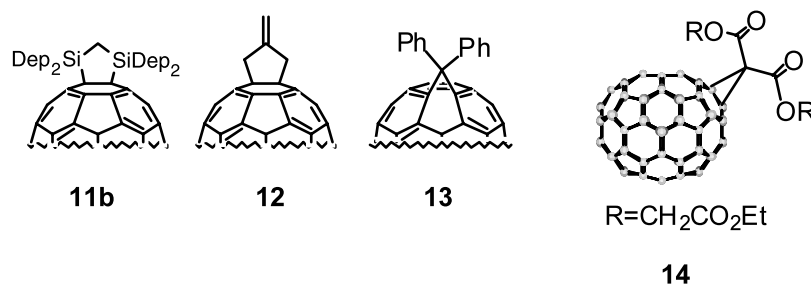
reduction potentials correlate better with the LUMO+1 energy levels. The oxidation potentials also show a good linear correlation with the HOMO energy levels. Silicon derivatives **2a** and **11b** are even more electropositive than their carbon analogs **12** and (diphenylmethano)fullerene **13** (Table 4) [12]. The reduction potentials depend on the electronegativities of the attached atoms. Electron-donating groups, such as alkyl and silyl, significantly lower the oxidation potential of C_{60}. This is in agreement with the calculations which indicate that almost one electron is transferred onto C_{60} from the silicon substituent.

The two silylated C_{70}s showed very similar redox properties even though the addition positions are different [13]. These results indicate that there exist no significant differences between the redox properties of these adducts having different addition positions. Diederich and coworkers also reported that the constitutional isomers of the multi-adducts of C_{70} displayed nearly identical redox properties [14]. As a general trend, the reductions become slightly more difficult, whereas the first oxidation becomes much more facilitated. The redox properties of bis(alkoxycarbonyl)methano–C_{70}(**14**), which is a carbon analogue of **9A**, was also recently reported [14]. It is impressive that the silicon derivative **9A** is even more electropositive than its carbon analogue **14**. These redox characteristics of the C_{70} adducts closely resemble those of the silylated C_{60}s [15].
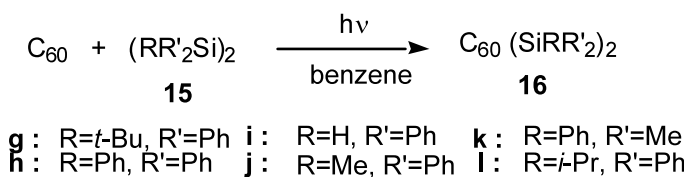
3. Silylation of fullerenes with silyl radical

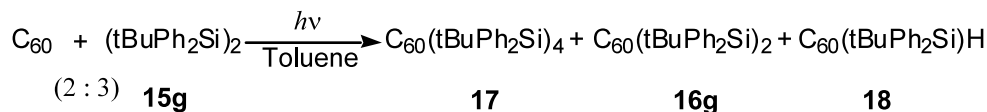### 3.1. Reaction of C_{60} with silyl radical from disilane

Irradiation of a benzene solution of 1,1,2,2-tetraphenyl-1,2-di-*tert*-butyl-1,2-disilane (**15g**) and C_{60} (1:1) with a low-pressure mercury-arc lamp resulted in formation of the adduct **16g** in high yield [16] (Scheme 3). The adduct **16g** can be readily isolated by preparative HPLC. Similar results were also obtained with hexaphenyldisilane (**15h**) and 1,1,2,2-tetraphenyldisilane (**15i**).

The NMR spectral data clearly indicate C_2 symmetry for **16g**. AM1 molecular orbital calculations [7] confirm the 1,6-adduct structure with C_2 symmetry for **16g** (1,16- or 1,29-addition product represented by the Schlegel diagram is named 1,6-adduct for convenience). The optimized structure of 1,6-(^{t}BuPh$_2$Si)$_2$C$_{60}$ at the AM1 level is shown in Fig. 1 [17].

The formation of **16g** might be rationalized in terms of the intermediacy of a ^{t}BuPh$_2$Si$^\bullet$ radical generated by

$$C_{60} \ + \ (RR'_2Si)_2 \ \xrightarrow[\text{benzene}]{h\nu} \ C_{60}(SiRR'_2)_2$$

15 **16**

g : R=*t*-Bu, R'=Ph **i** : R=H, R'=Ph **k** : R=Ph, R'=Me
h : R=Ph, R'=Ph **j** : R=Me, R'=Ph **l** : R=*i*-Pr, R'=Ph

Scheme 3.

$$C_{60} \; + \; (tBuPh_2Si)_2 \xrightarrow[\text{Toluene}]{h\nu} C_{60}(tBuPh_2Si)_4 + C_{60}(tBuPh_2Si)_2 + C_{60}(tBuPh_2Si)H$$

$$(2:3) \quad \textbf{15g} \hspace{6em} \textbf{17} \hspace{5em} \textbf{16g} \hspace{5em} \textbf{18}$$

Scheme 4.

photochemical Si–Si cleavage of **15g**. In fact, no **16g** was produced upon irradiation at > 300 nm where cleavage of **15g** does not occur. This radical mechanism [18] is further substantiated by control experiments in the presence of a radical scavenger (cumene and CCl_4). In contrast, no silylated C60 product was obtained in the photolysis of C_{60} with $(MePh_2Si)_2$ (**15j**), $(Me_2PhSi)_2$ (**15k**), and $(^iPrPh_2Si)_2$ (**15l**). These results of **15j–l** might be attributable to inhibition of silyl radical addition to C_{60} caused by the concomitant reactions such as disproportionation of silyl radicals and intramolecular 1,3-silyl migration.

Consequently, it has been demonstrated that bissilylation of C_{60} takes place readily via silyl radicals generated photochemically from some simple disilanes. Experimental data and theoretical calculations suggest that the redox properties of fullerenes (mentioned below) are controlled not only by the electronegativity of the substituents, but also by the regiochemistry of the functionality and its effect on their network. It is expected that these derivatized fullerenes, which display strikingly low oxidation potentials, will open up new applications of C_{60} as electron-donors. In this context, we recently obtained tetrakis-silylated C_{60} derivatives in a regioisomeric mixture, as shown below [19].

A photochemical reaction of C_{60} with disilane in a 2:3 ratio affords the isomer mixture of the tetrakis-adduct of $C_{60}(^tBuPh_2Si)_4$ (**17g**) [19] as the major product, accompanied with bis- (**16g**) [17] and mono-adduct (**18g**) [20] (Scheme 4). The use of a three-stage HPLC separation system isolated three of their isomers (**17A–C**). The ^1H- and ^{13}C-NMR measurements of **17A–C** reveal that these isomers have the C_{2h}, C_2 and C_1 symmetry, respectively [19].

The addition of two bulky $^tBuPh_2Si$ groups on the C_{60} cage at the 1,2- and 1,4- positions can be ruled out due to the steric hindrance [16]. Consequently, it could be undoubtedly considered that the 1,6-addition affords the tetrakis-adduct. The clue to understanding the structures of **17A–C** can be provided from the AM1 molecular orbital calculation [7] of several tetrakis-silylated C_{60} derivatives. Table 5 shows seven possible isomers of $C_{60}(^tBuPh_2Si)_4$ accompanied by the corresponding relative energy, symmetry and the number of double bonds at the 5,6-junction. Isomer **A** is found to be the most stable among these isomers. Although isomer **B** is 1.1 kcal mol^{-1} less stable than **A**, it is the most stable of the isomers which have C_2 symmetry. Isomer **C** is less stable than **A** and **B**, but **C** is more stable than **G**. On the basis of these observations, **17A–C** may correspond to isomers **A**, **B** and **C**, which have C_{2h}, C_2 and C_1 symmetries, respectively. Fig. 3 shows the Schlegel diagrams of isomers **A**, **B** and **C**.

3.2. Reaction of C_{70} with silyl radical from disilane

The reaction was carried out by the photoirradiation of a toluene solution of C_{70} and disilane **15g** (1:1 molar ratio) under a low-pressure mercury-arc lamp afforded bis-adducts, **19A** and **19B** as major products in moderate yields and mono-adducts, **20A–C** (Scheme 5) [21].

The ^1H- and ^{13}C-NMR measurements suggest that both bis-adducts, **19A** and **19B**, have C_1 symmetry.

Three mono-adduct isomers, **20A–C**, were also characterized on the basis of the ^1H-, ^{13}C-, and ^{29}Si-NMR and UV-absorption measurements. The spectral data suggest the C_s, C_1 and C_1 symmetries for **20A–C** isomer, respectively. **20A–C** are the 1,2-adducts at a–b, c–c and d–d position, respectively (Fig. 2).
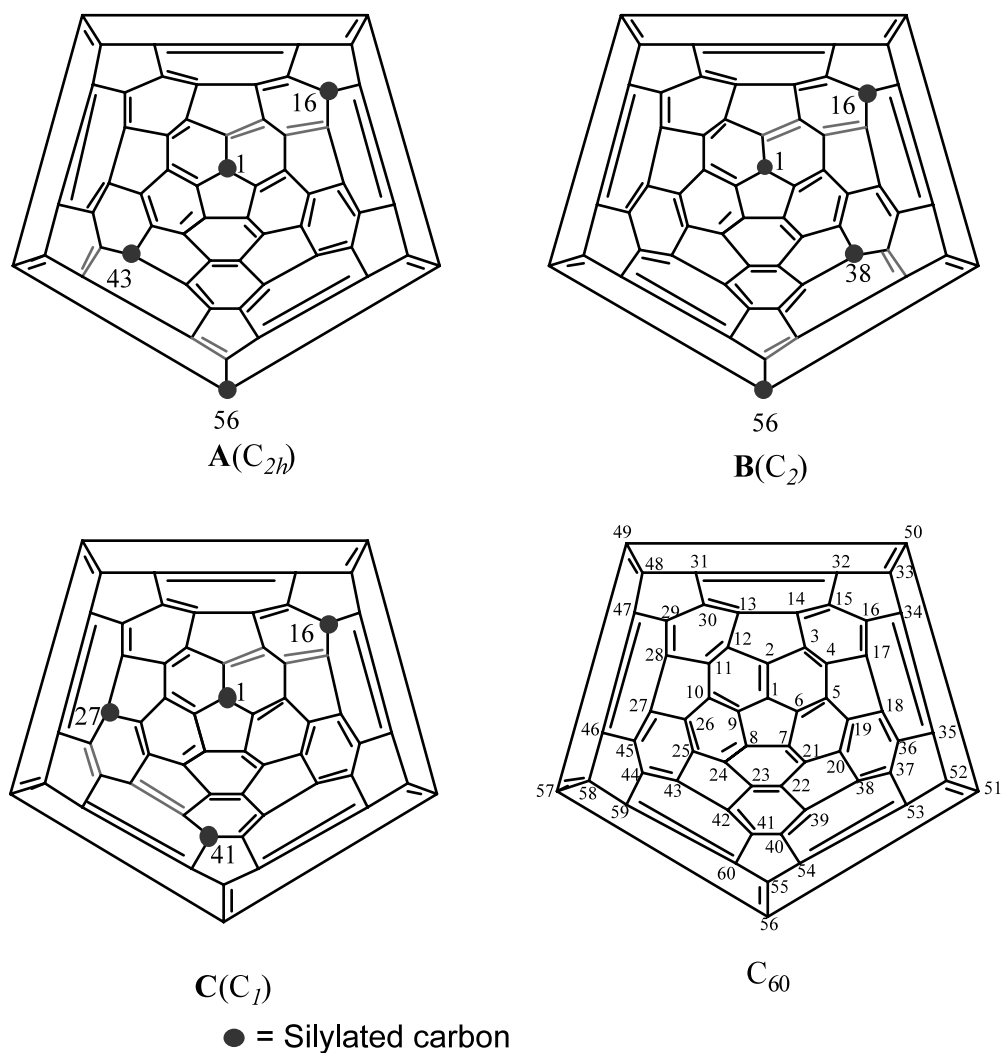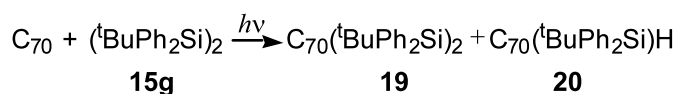
Table 5
The relative energies and the number of double bonds at 5,6-junction of possible tetrakis isomers

Isomer	Symmetry[a]	Number of double bond at 5,6-junction	Relative energy[b]
A (1, 16, 43, 56)	C_{2h}	4	0.0
B (1, 16, 38, 56)	C_2	4	1.1
C (1, 16, 27, 41)	C_1	4	4.7
D (1, 16, 39, 44)	C_2	4	9.6
E (1, 16, 23, 53)	C_2	4	11.2
F (1, 16, 42, 57)	D_2	4	12.8
G (1, 16, 25, 47)	C_1	4	15.3

[a] The symmetries with fee rotation of $Si(Ph_2^tBu)$ group.
[b] Calculated at the AM1 level.

● = Silylated carbon

Fig. 3. Schlegel diagram of tetrakis isomers A–C and C₆₀.

Scheme 5.

Table 6
Relative energies of $C_{70}H^a$ and $C_{70}SiH_3{}^b$ radical isomers in kcal mol^{-1}

Isomer	$C_{70}H^\bullet$		$C_{70}SiH_3{}^\bullet$
	PM3	BP	B3LYP
A	1.6	0.0	1.1
B	2.5	1.2	1.8
C	0.0	1.9	1.3
D	0.4	0.4	0
E	15.6	7.8	14.2

[a] Ref. [23e].
[b] Calculated at B3LYP/3-21G*//AM1 level.

In the reaction of C_{70} with **15g**, $^t\text{BuPh}_2\text{Si}$ radical must also play an important rule as well as the formation of $C_{60}(^t\text{BuPh}_2\text{Si})_2$ [16]. The initial step of this reaction is thought to be the addition of the $^t\text{BuPh}_2\text{Si}$ radical on the C_{70} cage. Since C_{70} has the five distinct carbon atoms, [22] a–e, radical addition to C_{70} can give rise to the isomeric adducts [23]. The theoretical calculations are carried out not only for the five $C_{70}SiH_3$ radical (A–E; named after the five carbons to which a radical can add.) but also for the five $C_{70}(SiH_3)_2$ to obtain the information about the structures of **19A** and **19B** (Tables 6 and 7). The unpaired spin densities of $C_{70}SiH_3$ radical isomers by population analysis are attributable to the difference on reactivity of these isomers depending on addition position of SiH_3 radical. Under consideration of the experimental data and theoretical calculations, it has been suggested that the bis-adducts, **19A** and **19B**, may correspond to the c–d and b–c isomer, respectively, though the exact assign-

Table 7
Symmetries, relative energies and HOMO, LUMO levels for the possible 1,6-$C_{70}(SiH_3)_2$ isomers

Adduct	Addition position[a]	Symmetry	Relative heat of formation[b]	HOMO	LUMO
a–e	2, 20	C_1	22.0	−8.54	−3.19
b–c	1, 16	C_1	4.2	−8.63	−3.18
c–d	5, 23	C_1	0	−8.70	−3.04
c–c	5, 40	C_2	24.5	−8.03	−3.52
d–e	7, 36	C_1	29.5	−8.28	−3.29

[a] Schlegel diagram's number.
[b] Calculated at the AM1 level.

C_{70}

3.3. Redox properties of silyl radical adducts

As shown in Tables 4 and 8, **16g** and the related bissilylated compounds **11b** (1,2-adduct), **21** (1,4-adduct) showed three reversible reductions and two irreversible oxidations in 1,2-dichlorobenzene [16]. The salient feature is that 1,6-adduct **16g** has a remarkably low oxidation potential (+0.33 V) compared with **11b** (+0.77 V) and **21b** (+0.73 V). The theoretical calculation (UHF/3-21G//AM1) [24] is in agreement with this result; the ionization potentials of $(H_3Si)_2C_{60}$ decrease in the order 1,2-adduct **22** (7.26 eV) > 1,4-adduct **22′** (7.09 eV) > 1,6-adduct **22″** (6.40 eV) as shown in Table 9. This

ment of the isomers, may await X-ray structural determination, because both isomers have C_1 symmetry. By the unique reactivity of $C_{70}SiH_3$ radical isomers, the reaction of C_{70} with disilane may cause formation of the monosilylated adducts, which is a contrast to that of C_{60} with disilane resulting in formation of mono silylated C_{60} only in trace amount [16].

dramatic result for the electrochemical properties can be explained by the unique structure of the 1,6-adduct; the 1,6-adduct has two short bonds between a pentagon and a hexagon, which gives more strain to the carbon framework (Fig. 4) [16]. This strain energy may be released in the cationic form where these bonds (1.450 Å by AM1) are much longer than those in the neutral form (1.387 Å by AM1). The CV analysis showed lower oxidation and higher reduction potentials when compared with $C_{60}(^tBuPh_2Si)_2$ and the parent C_{60}.

Table 8 also summarizes the redox behaviors of **17A–C** [19]. These isomers reveal very close oxidation and reduction potentials to each other, which may be due to the small energy differences among them. There are two salient features for the tetrakis-adduct isomers. (1) **17A–C** has lower oxidation potentials than any of the other silylated C_{60} derivatives. To the best of our knowledge, the silylated C_{60} derivatives show the lowest oxidation potentials of the previously reported C_{60}s [8,13]. These observations indicate that the four silyl groups on the fullerene cage are very effective for increasing the

Table 8
Redox potentials [V] of silyl radical adducts[a]

Compound	oxE2	oxE1	redE1	redE2	redE3
21	+1.26	+0.73	−1.22	−1.61	−2.12
16g	+1.20	+0.33	−1.19	−1.59	−2.18
17A	+0.38	+0.24	−1.20	−1.67	
17B	+0.04	+0.22	−1.41	−1.78	
17C	+0.41	+0.22	−1.24	−1.69	−2.19
19A	+1.23	+0.32	−1.20	−1.53	−2.03
19B	+1.17	+0.39	−1.26	−1.64	−2.09
20A	+1.18	+0.87	−1.12	−1.50	−2.00
20B	+1.11	+0.80	−1.09	−1.53	−1.98
20C	+1.12	+0.76	−1.07	−1.50	−2.03

[a] Values are relative to ferrocene/ferrocenium couple.
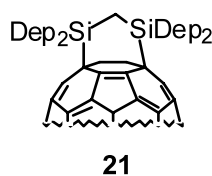
Table 9
The relative energies (kcal mol^{-1}) of **22**, **22'**, and **22''** and its cation radical, and ionization potentials (I_p, eV)[a]

Isomer	Neutral	Cation radical	Ip
1,2-Adduct **22**	3.4	7.4	7.26
1,4-Adduct **22'**	0	0	7.09
1,6-Adduct **22''**	14.5	−1.4	6.40

[a] Calculated at UHF/3-21G//AM1 level.

electron donor ability. (2) Although the bis-silylated fullerenes have only one low oxidation potential, the second oxidation potentials of **17A**–**C** are also very low. As mentioned above, the 1,6- bis-silylated fullerene **16g**, due to its unique structure, has a lower oxidation potential than that of the 1,2- or 1,4- bis-silylated compound. The 1,6-addition to the fullerene cage produces a highly strained dihydronaphthalene frame, where two short double bonds lie between the pentagon and the hexagon of the 1,6- adduct. This strain energy can be released in its cationic form. All the tetrakis-adducts **17** have two strained dihydronaphthalene frames on the fullerene cage. These dihydronaphthalene frames must exist independently, because the tetrakis-adduct **17** has two lower oxidation potentials. On the other hand, the reduction potentials of **17A**–**C** are cathodically shifted relative to **16g**, which suggests that the introduction of four silyl groups results in a decreasing electron-accepting property. These lower oxidation and higher reduction potentials are due to the influence of the four short double bonds on the C_{60} cage for each isomer as mentioned above.
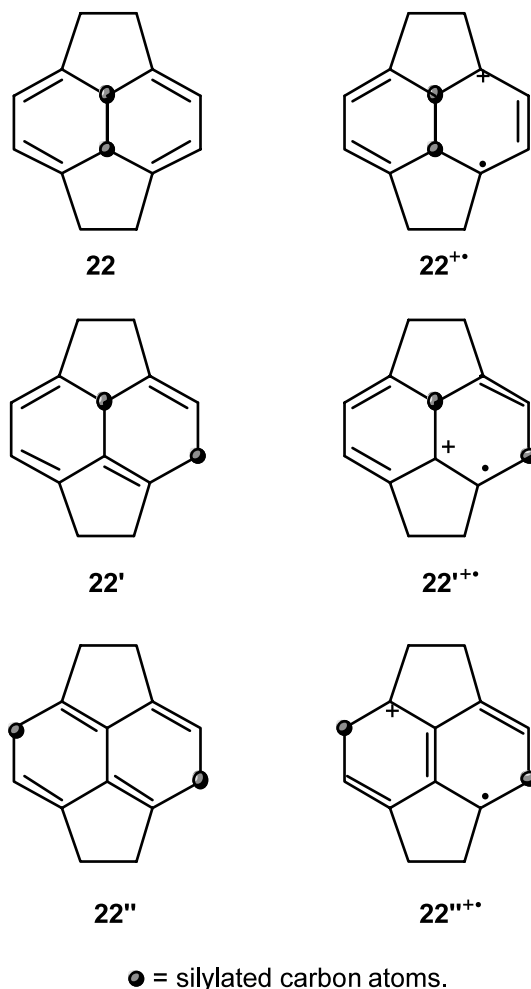

● = silylated carbon atoms.

Fig. 4. Selected bond lengths on neutral and cationic **22**, **22'**, and **22''** calculated by the AM1 method.

The electrochemical behaviors of **19A**, **19B**, **20A**–**C**, have been summarized in Table 8 [21]. The salient feature is that the first oxidation potentials of **19A** (+0.32 V) and **19B** (+0.39 V) are very unique as compare with **9A** (+0.59 V), **9B** (+0.61 V) and C_{70} (+1.21 V) (Table 4) itself. This unique electrochemical property was first observed in the C_{60} derivative **16g** and same trend also appeared in the silylated derivatives of C_{70}. The first oxidation potentials of mono-adducts, **20A**–**C**, are also considerably lower than parent C_{70}. This is an indication for the easier oxidation of bis- and mono-adducts than that of C_{70}.

3.4. Reaction of C_{60} with silyl radical from polysilane

Polysilanes, in which extensive delocalization of σ-electrons takes place along the silicon chain, have many interesting electronic properties and represent a unique class of materials [1]. It is well known that photolysis of polysilane with UV radiation leads to facile bond cleavage of the Si–Si bonds to afford the corresponding
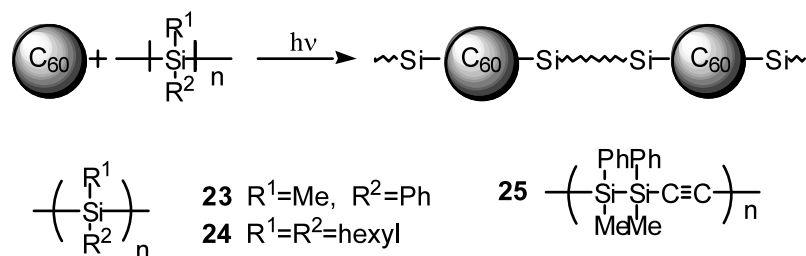
Scheme 6.
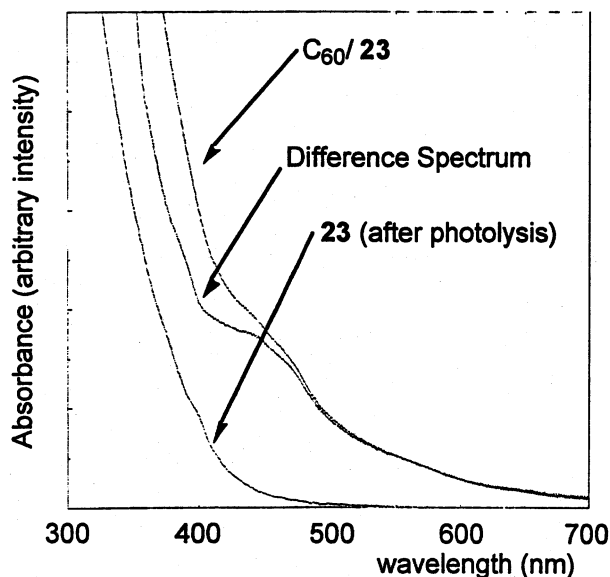
Fig. 5. UV–vis spectra of C60/**23**, **23** (after photolysis) and difference spectrum.

silyl radicals [1]. To extend the silylation reactions of C_{60}, we have carried out the photoreaction of polysilane with C_{60} to obtain a novel silicon polymer, which incorporates C_{60} into the polysilane chain [25].

A mixture of C_{60} and polysilanes **23**–**25** in benzene in a degassed quartz tube was photo-irradiated with a low-pressure mercury-arc lamp (Scheme 6) [25]. The reaction mixture was separated by gel permeation column chromatography to collect a high molecular weight polymer with absorption band above 400 nm (Fig. 5). This result suggests the incorporation of C_{60} in the polysilane chain, because the original polysilanes **23**–**25** have no absorption in this wavelength region. The molecular-weight of the adducts is higher than the those of irradiated polysilanes, indicating that C_{60} might act as a linker.

The mass spectra of C_{60}/polysilane adducts analyzed by FAB mass spectroscopy shows a C_{60} signal, which also confirms that C_{60} is incorporated in the polysilane chain [25]. Elemental analysis of the C_{60}/polysilane **23** adduct reveals that about 14% by weight of C_{60} is incorporated into the polysilane chain. Definitive evidence for a direct connection of the C_{60} and polysilane chain was gained from ^{13}C-NMR measurements of the adduct obtained from ^{13}C-enriched C_{60} and polysilane. A broad signal between 130 and 150 ppm in the ^{13}C-NMR, which is disappeared in the DEPT NMR spectrum, originated from the sp^2 carbons on the C_{60} skeleton reveals that C_{60} actually attaches to the polysilane chain. The ^{29}Si-NMR of C_{60}/polysilane **23** adduct indicates the existence of polysilane units in the C_{60}/polysilane **23** adduct.

The incorporation of C_{60} into polysilane was not observed upon irradiation at >300 nm, where the cleavage of Si–Si bond does not take place [25]. Formation of C_{60}/polysilane adduct was also suppressed by addition of CCl_4, which is known as a good silyl-radical scavenger. These results indicate that the formation of C_{60}/polysilane adduct can be rationalized in
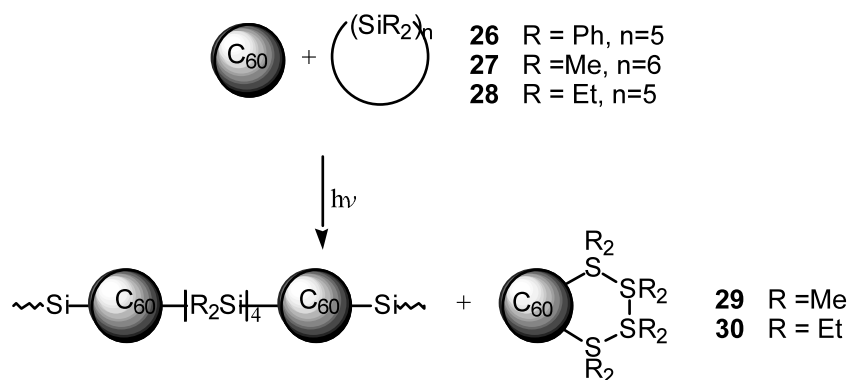
Scheme 7.

terms of the intermediacy of a silyl radical generated by photochemical Si–Si cleavage of polysilane.

In order to control the polysilane chain-length in C_{60}/polysilane adducts, the photoreaction of cyclic oligosilanes with C_{60} was carried out.(Scheme 7) [25]. A polymer obtained from C_{60} and cyclopentasilane **26** was separated. Elemental analysis shows about 38 wt% of C_{60} is incorporated into the polysilane chain. In the photoreaction of cyclohexasilane **27** and cyclopentasilane **28** with C_{60}, the high molecular weight fraction could not be collected, but $C_{60}(SiR_2)_4$ **29**(R = Me) and **30**(R = Et) were obtained after HPLC separation [26]. From the ^1H-, ^{13}C-NMR and UV–vis spectra, $C_{60}(SiR_2)_4$ has C_s symmetry and is a 1,4- addition product after fast ring inversion. It was reported that cyclohexasilane **27** formed $(SiMe_2)_4$ after extrusion of two silylenes (Me_2Si:) during UV irradiation, followed by a ring-opening reaction that results in formation of a 1,4-diradical [27]. The 1,4-diradicals reacted with C_{60} to give the adducts. These adducts may be good precursors for opening polymerization to produce new silicon/C_{60} polymers.

3.5. Properties of C_{60}—main chain polysilane

To learn the electronic properties of a C_{60}/polysilane adduct, its redox potentials were measured and compared with those of C_{60} and polysilane itself [25]. The C_{60}/**23** adduct has a lower oxidation potential (+0.77 V vs. Fc/Fc+ couple) than C_{60} (+1.21 V) and a lower reduction potential (−1.24 V) than polysilane (> −2 V). These data indicate that a C_{60}/polysilane adduct has unique electronic property.

It has been reported that C_{60} acts as a good dopant for photoconductive polymers [28]. Wang et al. reported that C_{60}-doped polysilane is a good photoconductor [28]. Electric conductivity of iodine-doped C_{60}/**23** (5×10^{-6} S cm^{-1}) is similar to that of the iodine-doped mixture of C_{60} and **23** (6×10^{-6} S cm^{-1}). The electric conductivity of the iodine-doped polysilane is 1×10^{-6} S cm^{-1}. These data reveal that C_{60} main chain polysilane has higher electric conductivity than the original polysilane. The photoconductivity measurement of the C_{60}/polysilane adduct is in progress.

The photochemical reaction of polysilanes and cyclic oligosilanes with C_{60} afforded C_{60}/polysilane adducts in which C_{60} was incorporated into a polysilane chain. The incorporation of C_{60} into polysilane could promise to open further extension of its application to new types of material.

4. Conclusion

Derivatization of fullerenes by the addition of active silicon compounds generated in photolysis of polysilanes has been developed. The silylated fullerenes have lower oxidation potentials than the parent fullerenes. These results indicate that silylation is very effective for producing the electronegatively fullerene derivatives. These silicon derivatives might constitute an important stepping stone on the way to the material, catalytic, and biological applications. It is expected that these silicon derivatives will constitute an important stepping-stone on the way to the material, catalytic, and biological applications.

References

[1] (a) R. West, in: S. Patai, Z. Rappoport (Eds.), The Chemistry of Organic Silicon Compounds (Part 2), Wiley, Chichester, UK, 1989, pp. 1207–1240 (Part 2);
(b) R.D. Miller, J. Michl, Chem. Rev. 89 (1989) 1359.
[2] (a) A. Hirsch, Fullerenes and Related Structures, Springer, Berlin, 1998;
(b) R. Taylor, The Chemistry of Fullerenes, World Scientific, 1995;
(c) A. Hirsch, The Chemistry of the Fullerenes, Thime Verlag, Stuttgart, 1994.
[3] For a recent review of silylfullerene, see: (a) T. Akasaka, T. Wakahara, S. Nagase, K. Kobayashi, J. Synth. Org. Chem. Jpn. 58 (2000) 1066. (b) W. Ando, T. Kusukawa, in: Z. Rappoport, Y. Apeloig (Eds.), In the Chemistry of Organic Silicon Compounds, Part 2, 2nd ed., Wiley, New York, 1998, pp. 1929–1960.
[4] For a recent review of silylenes, see: P.P. Gasper, R. West, In: Z. Rappoport, Y. Apeloig (Eds.), The Chemistry of Organic Silicon Compounds, Part 3, 2nd ed., Wiley, New York, 1999, pp. 2463–2568.
[5] T. Akasaka, W. Ando, K. Kobayashi, S. Nagase, J. Am. Chem. Soc. 115 (1993) 1605.
[6] W. Ando, M. Fujita, H. Yoshida, A. Sekiguchi, J. Am. Chem. Soc. 100 (1988) 3310 (and references cited therein).
[7] M.J. Dewar, C.X. Jie, Organometallics 6 (1987) 1486.
[8] M. Weidenbruch, Coord. Chem. Rev. 130 (1994) 275.
[9] T. Akasaka, E. Mitsuhida, W. Ando, K. Kobayashi, S. Nagase, J. Chem. Chem. Commun. (1995) 1529.
[10] T. Akasaka, E. Mitsuhida, W. Ando, K. Kobayashi, S. Nagase, J. Am. Chem. Soc. 116 (1994) 2627.
[11] G.E. Scuseria, Chem. Phys. Lett. 18 (1991) 451.

[12] T. Suzuki, Y. Maruyama, T. Akasaka, W. Ando, K. Kobayashi, Y. Nagase, J. Am. Chem. Soc. 116 (1994) 12232.

[13] T. Wakahara, A. Han, Y. Niino, Y. Maeda, T. Akasaka, T. Suzuki, K. Yamamoto, M. Kako, Y. Nakadaira, K. Kobayashi, S. Nagase, J. Mater. Chem. 12 (2002) 2061.

[14] C. Boudon, J.-P. Gisselbrecht, M. Gross, A. Herrman, M. Rüttimann, J. Crassous, F. Cardullo, L. Echegoyen, F. Diederich, J. Am. Chem. Soc. 120 (1998) 7860.

[15] We recently found that the bissilylations of the higher fullerenes are very effective for producing the electronegatively fullerene derivatives. (a) A. Han, T. Wakahara, Y. Maeda, Y. Niino, T. Akasaka, K. Yamamoto, M. Kako, Y. Nakadaira, K. Kobayashi, S. Nagase, Chem. Lett. (2001) 974. (b) T. Wakahara, A. Han, Y. Maeda, Y. Niino, T. Akasaka, K. Yamamoto, M. Kako, Y. Nakadaira, K. Kobayashi, S. Nagase, ITE Lett. 2 (2001) 649.

[16] T. Akasaka, T. Suzuki, Y. Maeda, M. Ara, T. Wakahara, K. Kobayashi, S. Nagase, M. Kako, Y. Nakadaira, M. Fujitsuka, O. Ito, J. Org. Chem. 64 (1999) 566.

[17] T. Kusukawa, W. Ando, Angew. Chem. Int. Ed. Engl. 35 (1996) 1315.

[18] (a) T. Kusukawa, A. Shike, W. Ando, Tetrahedron 52 (1996) 4995;
(b) T. Kusukawa, W. Ando, Organometallics 16 (1997) 4027;
(c) T. Kusukawa, W. Ando, J. Organomet. Chem. 559 (1998) 11.

[19] Y. Maeda, G.M.A. Rahman, T. Wakahara, M. Kako, S. Sato, M. Okamura, T. Akasaka, K. Kobayashi, S. Nagase, submitted for publication.

[20] T. Wakahara, G.M.A. Rahman, Y. Maeda, M. Kako, S. Sato, M. Okamura, T. Akasaka, K. Kobayashi, S. Nagase, ITE Lett. 4 (2003) C24.

[21] G.M.A. Rahman, Y. Maeda, T. Wakahara, M. Kako, S. Sato, M. Okamura, T. Akasaka, K. Kobayashi, S. Nagase, ITE Lett. 4 (2003) C17.

[22] H.R. Karfunkel, A. Hirsch, Angew. Chem. Int. Ed. Engl. 31 (1992) 1468.

[23] (a) I.D. Reid, E. Roduner, Hyperfine Interact. 86 (1994) 809;
(b) P.N. Keizer, J.R. Morton, K.F. Preston, J. Chem. Soc. Chem. Commun. (1992) 1259.;
(c) R. Borghi, L. Lunazzi, G. Placucci, P.J. Krusic, D.A. Dixon, N. Matsuzawa, M. Ata, J. Am. Chem. Soc. 118 (1996) 7608;
(d) B.L. Tumanskii, V.V. Bashilov, O.G. Kalina, V.I. Sokolov, J. Organomet. Chem. 599 (2000) 28;
(e) M.S. Meier, G.-W. Wang, R.C. Haddon, C.P. Brook, M.A. Lloyd, J.P. Selegue, J. Am. Chem. Soc. 120 (1998) 2337.

[24] GAUSSIAN 94, Gaussian, Inc., Pittsburgh, 1995.

[25] T. Wakahara, T. Kondo, M. Okamura, T. Akasaka, Y. Hamada, T. Suzuki, M. Kako, Y. Nakadaira, J. Organomet. Chem. 611 (2000) 78.

[26] T. Kusukawa, Y. Kabe, W. Ando, Organometallics 14 (1995) 2142.

[27] M. Ishikawa, M. Kumada, Adv. Organomet. Chem. 19 (1981) 51.

[28] Y. Wang, R. West, C.-H. Yuan, J. Am. Chem. Soc. 115 (1993) 3844 (and references cited therein).